Rev. LatinAm. Metal. Mat.

Artículo Regular

www.rlmm.org

PREPARATION, CRYSTAL STRUCTURE, THERMAL ANALYSIS, SCANNING ELECTRON MICROSCOPY AND OPTICAL BAND-GAPS OF Cu_2GeTe_4 AND Cu_2SnTe_4 ALLOYS

Pedro Grima-Gallardo[1], Ricardo Peña[1], Luis Nieves[1], Gustavo Marcano[1], Miguel Quintero[1], Ekadink Moreno[1], Jian-Han Zhang[2], Jacilynn A. Brant[2] & Jennifer A. Aitken[2]*

1: Centro de Estudios en Semiconductores (C.E.S.). Departamento de Física, Facultad de Ciencias, Universidad de Los Andes, Mérida 5101, Venezuela. 2: Department of Chemistry and Biochemistry, Duquesne University, Pittsburgh, Pennsylvania 15282, USA.

**e-mail: peg@ula.ve*

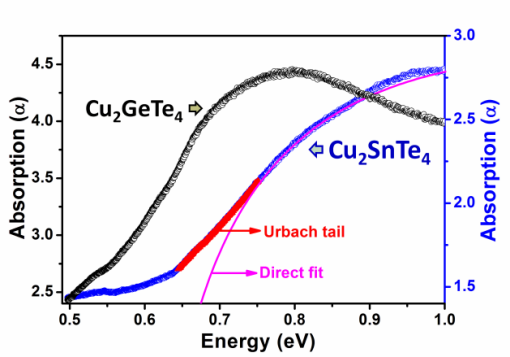

ABSTRACT

Polycrystalline samples (weight ~ 1g) of Cu_2GeTe_4 and Cu_2SnTe_4 alloys were prepared by the usual melt and anneal method and the products characterized by X-Ray Diffraction (XRD), Differential Thermal Analysis (DTA), Scanning Electron Microscopy (SEM) and Optical Diffuse Reflectance UV/VIS/NIR Spectroscopy techniques. It was found that: a) Cu_2GeTe_4 and Cu_2SnTe_4 crystallize in an orthorhombic structure (s.g. Imm2; N° 44) with lattice parameters a=5.9281(4) Å, b=4.2211(6) Å, c=12.645(5) Å and a=6.0375(6) Å, b= 4.2706 (3) Å, c=12.844(1) Å, respectively; b) both alloys show two thermal transitions: 762 and 636K upon heating and; 700 and 578K upon cooling for Cu_2GeTe_4; 702 and 636K upon heating and; 650 and 590K upon cooling for Cu_2SnTe_4; c) both alloys present large deviations of stoichiometry for the cations Cu (~35%), Ge (7.2%) and Sn (26.4%) and minor deviation within the experimental error, for the anion Te; and, d) the measured optical band gaps were 0.63 and 0.53 eV for Cu_2SnTe_4 and Cu_2GeTe_4, respectively.

Keywords: Semiconductor alloys, X-Ray Diffraction, Differential Thermal Analysis (DTA), Scanning Electron Microscopy (SEM), Optical Diffuse Reflectance UV/VIS/NIR Spectroscopy, Cu_2GeTe_4 and Cu_2SnTe_4

PREPARACION, ESTRUCTURA CRISTALINA, ANALISIS TERMICO, MICROSCOPIA ELECTRONICA DE BARRIDO Y BRECHA OPTICA DE ENERGIA DE LAS ALEACIONES Cu_2GeTe_4 Y Cu_2SnTe_4

RESUMEN

Se prepararon muestras policristalinas (peso ~ 1 g) de las aleaciones Cu_2GeTe_4 y Cu_2SnTe_4 por el método de fusión y recocido y los productos caracterizados por las técnicas de Difracción de Rayos X (DRX) , Análisis Térmico Diferencial (ATD), Microscopía Electrónica de Barrido (MEB) y espectroscopía de reflectancia óptica difusa UV / VIS / CIR. Se encontró que : a) Cu_2GeTe_4 y Cu_2SnTe_4 cristalizan en una estructura ortorrómbica (g.e. Imm2; N° 44) con parámetros de red a = 5,9281 (4) Å , b = 4.2211 (6) Å , c = 12.645 (5) Å y a = 6.0375 (6) Å , b = 4,2706 (3) Å , c = 12.844 (1) Å , respectivamente ; b) ambas aleaciones muestran dos transiciones térmicas : 762 y 636K al calentar y ; 700 y 578K tras el enfriamiento para Cu_2GeTe_4 ; 702 y 636K al calentar y ; 650 y 590K tras el enfriamiento para Cu_2SnTe_4 ; c) ambas aleaciones presentan importantes desviaciones estequiométricas en sus cationes: Cu (~35%), Ge (7.2%) and Sn (26.4%) y menor que el error experimental para el anión Te; y d) las brechas ópticas de energía medidas fueron 0.63 y 0.53 eV para Cu_2SnTe_4 y Cu_2GeTe_4, respectivamente.

Palabras Claves: Aleaciones semiconductoras, Difracción de Rayos X (DRX), Análisis Térmico Diferencial (ATD),Microscopía Electrónica de Barrido (MEB), Espectrocopía de Reflectancia Óptica Difusa, Cu_2GeTe_4 y Cu_2SnTe_4

1. INTRODUCTION

The Cu_2-IV-VI_3 and Cu_2-IV-VI_4 alloys (IV: Ge, Sn; VI: Se, Te) belong to the general Cu-IV-VI system and are located on the $(Cu_2IV)_{1-x}VI_x$ tie line, at x=3/4 and x=4/5, respectively, as it is showed in Figure 1. These alloys are candidates for applications in solar cells, thermoelectrics conversion and electro-optic devices [1-11].

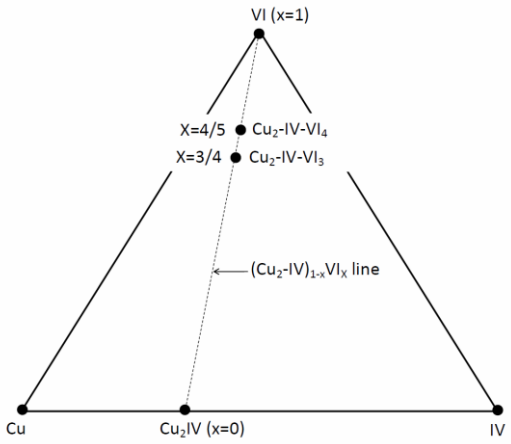

Figure 1. Representation of the Cu-IV-Te alloys system, indicating the localization of Cu_2-IV-VI_3 and Cu_2-IV-VI_4 alloys.

Recently, our group [12] has investigated the $Cu_2(Ge_{1-x}Sn_x)Se_4$ alloys system and determined that Cu_2GeSe_4 and Cu_2SnSe_4 crystallize in orthorhombic and cubic structures, respectively. The crystal system and lattice parameters of Cu_2GeSe_4 coincide with the high-temperature phase of Cu_2GeSe_3, whereas the cubic phase of Cu_2SnSe_4 coincides with the room temperature cubic phase of Cu_2SnSe_3. According to the phase diagram of the $(Cu_2Ge)_{1-x}(Se)_x$ tie line (Berger et al [13]; also see Figure 8 in [12]) the region in the composition range $3/4 \leq x \leq 4/5$ is single phase, i.e. Cu_2GeSe_3 and Cu_2GeSe_4 have the same crystal structure. However, there is a problem with this phase diagram: Cu_2GeSe_3 has a solid-to-solid phase transition at high temperature from the tetragonal structure (labeled as τ_1 in the phase diagram) to an orthorhombic structure (that henceforth we will call τ_2) that has not been taken into account in the diagram.

The analogous tellurium systems have also been studied. The structural properties of the Cu_2GeTe_3 alloy have been recently published by Delgado *et al* [14] and Villarreal *et al* [15] with the observation of an orthorhombic crystal structure, crystallizing in the space group Imm2 (N^o44), with lattice parameters a=5.9261(2)Å, b=4.2115(2)Å, and c=12.641(1)Å; on the other hand, the preparation and crystal structure of Cu_2SnTe_3 has been published by Delgado *et al* [16] who also reported an orthorhombic crystal structure in the space group Imm2 (N^o44), with lattice parameters a=6.043(1)Å, b=4.274(1)Å, and c=12.833(4)Å. Previously, Sharma *et al* (1977) [17] reported that Cu_2GeTe_3 and Cu_2SnTe_3 are two-phases solids with eutectic type microstructure; for Cu_2GeTe_3 they found a tetragonal structure with lattice parameters a=5.959Å and c=11.858Å and for Cu_2SnTe_3 a cubic disordered structure, with lattice parameter a=6.094Å.

From thermal analysis, Dovletov *et al* [18] reported that no ternary compounds were found in the Cu_2Te-SnTe binary system, but Palatnik *et al* (1961) [19], Rivet *et al* (1963) [20], Averkieva *et al* (1965) [21], Rivet *et al* (1965) [22] and Carcaly *et al* (1975) [23], (1977) [24] affirm the existence of a ternary phase which forms peritectically at 780-785K.

In this work we report the preparation and characterization of polycrystalline samples of Cu_2GeTe_4 and Cu_2SnTe_4.

2. EXPERIMENTAL PART

2.1 Preparation

Cu_2GeTe_4 and Cu_2SnTe_4 were synthesized using the melt and anneal technique. Stoichiometric quantities of Cu, Ge, Sn and Te elements with purity of 99.99% were charged in an evacuated synthetic silica glass ampoule, which was previously subjected to pyrolysis in order to avoid reaction of the starting materials with silica glass. Then, the ampoule was sealed under vacuum (~10^{-4} Torr) and the fusion process was carried out inside a furnace (vertical position) heated up to 1500K at a rate of 20K/h, with a stop of 48 h at 722.5K (melting temperature of Te) in order to maximize the formation of binary species at low temperature and minimize the presence of unreacted Te at high temperatures. The ampoule was shaken using a mechanical system during all the heating process in order to help the complete mixing of all the elements. The maximum temperature (1500K) was kept for other 48 hours with the mechanical shaking system on. Then, the mechanical shaking system was turning off and the temperature was gradually lowered, at the same rate of 20K/h, until 873K. The

ampoule was held at this temperature for a period of 30 days. Finally, the sample was cooled to room temperature at a rate of 10K/h. The obtained ingots were bright gray in color and homogeneous to the eye.

2.2 X-Ray Powder Diffraction

A small amount of each compound was gently ground in an agate mortar and sieved to a grain size of less than 38 μm. Each sample was mounted on a zero-background specimen holder for the respective measurement. X-ray powder diffraction patterns of the samples were recorded using a D8 FOCUS BRUKER diffractometer operating in Bragg-Brentano geometry and equipped with a copper X-ray tube (CuKα radiation: λ=1.5406 Å, 40 kV and 40 mA) using a nickel filter and one the dimensional LynxEye detector. A fixed antiscatter slit of 8 mm, receiving slit of 1 mm, soller slits of 2.5° and a detector slit of 3 mm were used for the diffraction optics. Data were collected from 2 to 140° (2θ) with a step size of 0.02° (2θ) and a counting time of 0.4 s/step.

2.3 Differential Thermal Analysis

Phase transition temperatures were obtained from differential thermal analysis (DTA) measurements, in the temperature range of 300 to 1500K, using a Perkin-Elmer DTA-7. The instrument was calibrated using aluminum and gold as references. The charge was a powdered alloy of approximately 100-mg in weight. Both heating and cooling runs were carried out on each sample, the average rates of these runs were approximately 10 K/min. The error in determining these temperatures is about ±10K. The temperature values of the thermal transitions were obtained using the intercept of the base line with the beginning of the corresponding peak.

2.4 Scanning Electron Microscopy (SEM) and Energy Dispersive Spectroscopy (EDS)

SEM/EDS was performed on a Hitachi S-3400N scanning electron microscope equipped with a Bruker Quantax model 400 energy dispersive spectrometer using an XFlash® 5010 EDS detector with a 129 eV resolution. Samples were mounted on double-sided carbon tape affixed to an aluminum specimen holder. EDS spectra were collected using a working distance of 10 mm and an accelerating voltage of 15 kV for 3 min live time.

2.5 Optical Diffuse Reflectance UV/VIS/NIR Spectroscopy

Optical diffuse reflectance spectra of the Cu_2GeTe_4 and Cu_2SnTe_4 were obtained using a Varian Cary 5000 UV/VIS/NIR spectrometer equipped with a Harrick Praying Mantis diffuse reflectance accessory that uses elliptical mirrors. Each sample was ground and placed into a sample holder to a depth of 3 mm. Barium sulfate (Fisher, 99.92%) was used as a 100% reflectance standard. Data were collected from 2500 to 200 nm at a scan rate of 600 nm/min. Using the Kubelka-Munk transformation, $\alpha_{KM} / s = (1-R)^2/(2R)$, the raw reflectance (R) was converted to a relative absorption (α_{KM}) since the scattering coefficient, *s*, is unknown [25]. The Urbach energy was also obtained by fitting the optical data to the functional form $\alpha = A \exp(E-E_g/E_u)$, where A is a constant, E is the photon energy in eV, E_g is the band gap energy, and E_u is the Urbach energy [26].

3. RESULTS AND DISCUSSION

In Figures 2 and 3, the experimental X-ray powder diffraction patterns of Cu_2GeTe_4 and Cu_2SnTe_4 are displayed. Sharp diffraction peaks were observed in the range of 20-140° 2Θ indicating good crystallinity and that the samples had reached thermal equilibrium during synthesis.

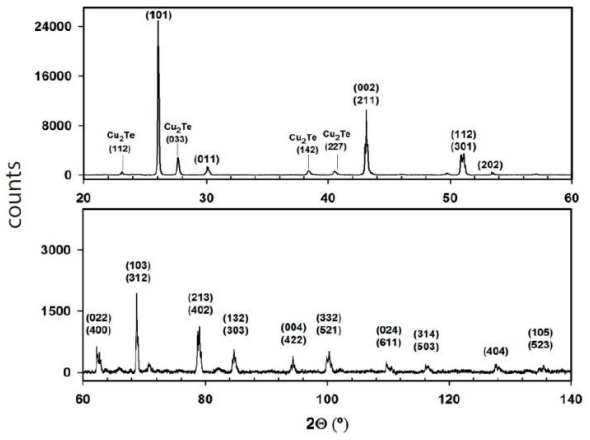

Figure 2. Diffraction pattern of the alloy Cu_2GeTe_4. The hkl-Miller indices are labeled on the top of each peak. A secondary phase, identified as Cu_2Te was also observed.

For both alloys, the diffraction patterns can be fully indexed with two phases: one with the orthorhombic crystal structure, space group Imm2, N° 44, Z=2, and a secondary one identified as Cu_2Te. The lattice

parameters (Tables I and II) were calculated using the software Dicvol04 [27]. Those obtained for the orthorhombic phase are very close with those reported previously for the analogous ternaries Cu_2GeTe_3 and Cu_2SnTe_3 [2-4] (see Table III).
With respect to the secondary phase, Cu_2Te does not belongs to the $(Cu_2Ge)_{1-x}Te_x$ or $(Cu_2Ge)_{1-x}Te_x$ tie lines, so it is probable that the mechanical shaking during the heating process was not enough to dissolve it.

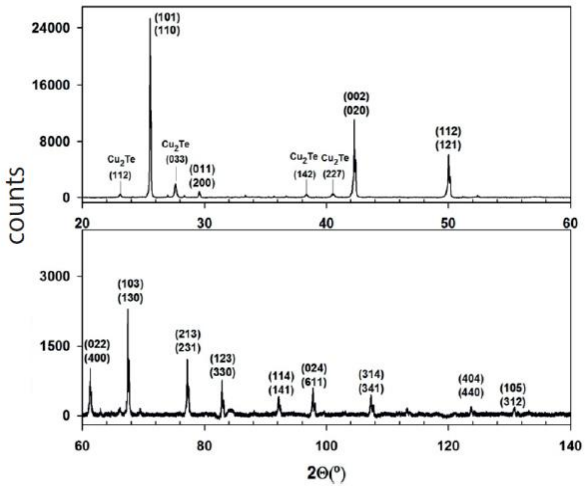

Figure 3. Diffraction pattern of the alloy Cu_2SnTe_4. The hkl-Miller indices are labeled on the top of each peak. A secondary phase, identified as Cu_2Te was also observed.

DTA measurements are showed in Figure 4. Two thermal transitions are observed for both alloys, Cu_2GeTe_4 and Cu_2SnTe_4. In the case of Cu_2GeTe_4, the thermogram shows, transitions occurring at 762 and 636K in the heating cycle, and transitions at 700 and 578K in the cooling cycle. Thermal transitions for Cu_2SnTe_4 were observed at 702 and 636K upon heating and 650 and 590K upon cooling. It is evident that the overheating (or supercooling) effect produces the positive difference of $(T_f - T_s)$ where T_f and T_s are the fusion and solidification temperatures, respectively.

The first thermal event corresponds to the solid-to-solid transition, i.e. from the room temperature (tetragonal?) to the high temperature phase (orthorhombic?), and the second thermal event correspond to the melting (or solidification) of the solid (liquid) phase. The shape of the peaks in the cooling cycle suggests that the sequence of transitions for Cu_2GeTe_4 are liquid-solid$_1$-solid$_2$, whereas for Cu_2SnTe_4 are liquid-solid$_1$+liquid-solid$_2$.

The well-known Grimm-Sommerfeld condition for semiconductors, states that a compound must have an average of 4 valence electrons per atom. In the case of Cu_2GeTe_4 and Cu_2SnTe_4, Cu is bivalent (Cu^{+2}), Ge (or Sn) is tetravalent (Ge^{+4} or Sn^{+4}) and Te is hexavalent (Te^{+6}). The sum gives 32 electrons in total. However, there are only seven atoms (2Cu + 1 Ge + 4 Te); therefore, it is necessary to have a vacancy in the crystal structure in order to have a total 8 "atoms" for the 32 electrons, giving an average of 4 electrons per atom. Thus, the formula units must be written as □-Cu_2GeTe_4 and □-Cu_2SnTe_4.

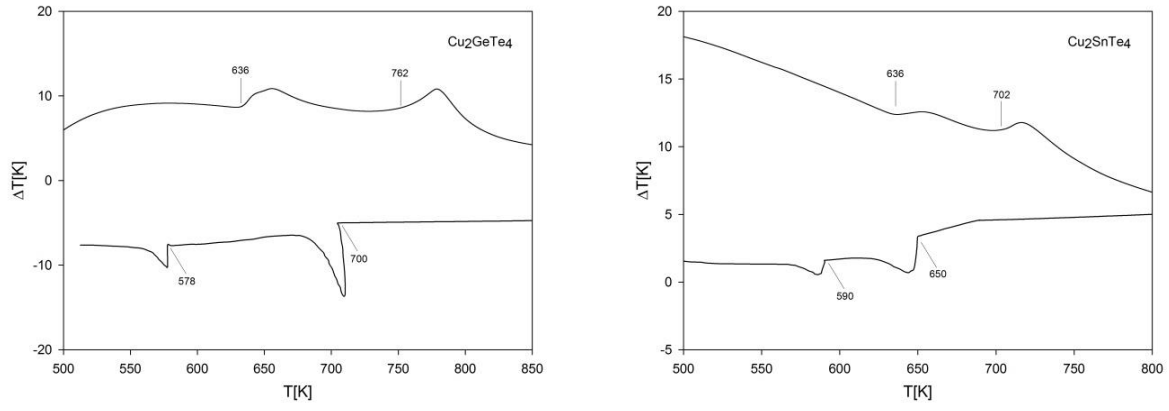

Figure 4. DTA curves of Cu_2GeTe_4 (left) and Cu_2SnTe_4 (right). Top curves: heating cycle; bottom curves: cooling cycle. The labels show the transition temperatures.

Table I. Indexation of Cu_2GeTe_4.

Orthorhombic, space group Imm2 (N^o 44), Z=2
***Lattice parameters**: a=5.9281(4) Å, b=4.2211(6) Å, c=12.645(5)Å*

$2\Theta_{obs}(^o)$	d_{obs} (Å)	I/I_0	hkl	$2\Theta_{cal}(^o)$	d_{cal} (Å)	$\Delta 2\Theta(^o)$
25.916	3.43519	100.0	101	25.911	3.43591	0.006
29.933	2.98268	5.5	011	29.929	2.98314	0.005
42.858	2.10839	17.1	002	42.873	2.10772	-0.014
42.983	2.10257	41.1	211	42.980	2.10270	0.003
50.793	1.79606	12.9	112	50.765	1.79700	0.029
50.980	1.78993	14.1	301	50.997	1.78937	-0.017
53.289	1.71768	1.9	202	53.287	1.71774	0.002
62.188	1.49154	2.6	022	62.195	1.49140	-0.006
62.613	1.48245	1.7	400	62.626	1.48216	-0.013
68.593	1.36705	3.7	103	68.585	1.36719	0.008
68.763	1.36409	8.0	312	68.754	1.36424	0.008
78.640	1.21566	4.1	213	78.626	1.21584	0.014
78.861	1.21280	4.4	402	78.895	1.21236	-0.034
84.285	1.14803	1.1	132	84.279	1.14810	0.006
84.526	1.14537	2.0	303	84.550	1.14511	-0.024
93.936	1.05380	0.7	004	93.940	1.05377	-0.004
94.231	1.05128	1.4	422	94.233	1.05126	-0.002
99.805	1.00699	1.4	332	99.815	1.00692	-0.010
100.198	1.00410	2.0	521	100.215	1.00398	-0.017
109.579	0.94280	0.7	024	109.581	0.94278	-0.002
110.436	0.93787	0.6	611	110.425	0.93793	0.011
116.062	0.90801	0.7	314	116.055	0.90805	0.007
116.462	0.90605	0.6	503	116.444	0.90613	0.018
127.496	0.85889	0.7	404	127.519	0.85880	-0.023
134.728	0.83459	0.4	105	134.726	0.83460	0.002
135.389	0.83260	0.8	523	135.379	0.83263	0.010

Figure of Merit: M(26)= 41.3; F(26)=19.0(0.0099, 138) [27]

Table II. Indexation of Cu_2SnTe_4.

Orthorhombic, space group Imm2 (N^o 44), Z=2
***Lattice parameters**: a= 6.0375(6) Å, b= 4.2706 (3) Å, c=12.844(1)Å*

$2\Theta_{obs}(^o)$	d_{obs} (Å)	I/I_0	hkl	$2\Theta_{cal}(^o)$	d_{cal} (Å)	$\Delta 2\Theta(^o)$
25.539	3.48503	100.0	101	25.549	3.48372	-0.010
25.598	3.47719	48.1	110	25.549	3.48372	0.049
29.571	3.01841	3.4	011	29.584	3.01711	-0.013
29.649	3.01063	1.8	200	29.632	3.01234	0.017
42.255	2.13710	43.7	002	42.245	2.13756	0.010
42.364	2.13183	21.3	020	42.357	2.13218	0.007
50.016	1.82214	24.1	112	50.018	1.82206	-0.002
50.149	1.81763	12.1	121	50.092	1.81956	0.057
61.281	1.51142	3.9	022	61.330	1.51034	-0.049
61.438	1.50795	2.1	400	61.438	1.50795	0.000
67.438	1.38764	9.1	103	67.435	1.38768	0.002
67.609	1.38453	4.7	130	67.618	1.38437	-0.009
77.207	1.23460	4.8	213	77.236	1.23420	-0.030
77.428	1.23163	2.5	231	77.390	1.23213	0.038
82.872	1.16398	3.0	123	82.913	1.16350	-0.041
83.113	1.16121	1.3	330	83.093	1.16144	0.020
92.143	1.06956	1.6	004	92.120	1.06976	0.023
92.444	1.06686	0.9	040	92.421	1.06707	0.024
97.768	1.02246	2.4	114	97.736	1.02271	0.032
98.069	1.02012	1.1	141	98.020	1.02050	0.049
107.268	0.95660	1.6	024	107.291	0.95646	-0.023
107.623	0.95443	0.6	611	107.632	0.95438	-0.009
113.250	0.92242	0.6	314	113.265	0.92234	-0.015
113.602	0.92056	0.4	341	113.571	0.92072	0.031
123.898	0.87283	0.3	404	123.897	0.87284	0.001
124.256	0.87139	0.4	440	124.259	0.87137	-0.003
130.695	0.84755	0.5	105	130.690	0.84757	0.005
131.309	0.84548	0.4	150	131.310	0.84548	-0.001

Figure of Merit: M(28)= 29.0; F(28)= 14.9(0.0134, 140) [27]

Table III. Comparison of the obtained lattice parameters for the alloys Cu_2GeTe_4 and Cu_2SnTe_4 with Cu_2GeTe_3 and Cu_2SnTe_3.

	Lattice parameters	*Crystal Structure*	*References*
Cu_2GeTe_4	a=5.9281(4) Å, b=4.2211(6) Å, c=12.645(5)Å V=316.42Å^3	Orthorhombic	This work
Cu_2GeTe_3	a=5.9261(2) Å, b=4.2115(2) Å, c=12.641(1)Å V=315.49Å^3	Orthorhombic	[14-15]
Cu_2GeTe_3	a=5.959Å, c=11.858Å V=421.07Å^3	Tetragonal	[17]
Cu_2SnTe_4	a= 6.0375(6) Å, b= 4.2706 (3) Å, c=12.844(1)Å V=331.17Å^3	Orthorhombic	This work
Cu_2SnTe_3	a= 6.043(1) Å, b= 4.274 (1) Å, c=12.833(4)Å V=331.45Å^3	Orthorhombic	[16]
Cu_2SnTe_3	a=6.094Å V=226.31Å^3	Cubic (disordered)	[17]

Table IV. Thermal transition values for Cu_2GeTe_4 and Cu_2SnTe_4

	Heating [K]	*Cooling [K]*	*Remarks*
Cu_2GeTe_4	762 and 636	700 and 578	Cu_2GeTe_3 M_p: 800K [14]; 777K[3]
Cu_2SnTe_4	702 and 636	650 and 590	Cu_2SnTe_3: 655K [5]

Table V. Comparison of experimental and nominal stoichiometry of the alloys Cu_2GeTe_4 and Cu_2SnTe_4.

Cu_2GeTe_4	*Nominal [at%]*	*Experimental [at%]*	*Deviation [%]*	*Cu_2SnTe_4*	*Nominal [at%]*	*Experimental [at%]*	*Deviation [%]*
Cu	25.0	34.4	+37.6	Cu	25.0	33.8	+35.2
Ge	12.5	13.4	+7.2	Sn	12.5	15.8	+26.4
Te	50.0	52.2	+4.4	Te	50.0	50.4	+0.8

Scanning electron microscopy (SEM) coupled with energy dispersive spectroscopy was used to compare the experimental composition to the nominal stoichiometry. For Cu_2GeTe_4, measurements were performed in three different points of the sample while for Cu_2SnTe_4 data were collected on four points. The results are displayed in Table V where the column "experimental" represents the mean value of all measurements for each sample.

We observe stoichiometric deviations that are larger than the experimental error generally accepted for this technique which is ~ 10%. Moreover, both alloys show a coincidence of ~35% excess Cu which discards any experimental error. Cu_2GeTe_4 has a Ge-excess of 7.2% whereas Cu_2SnTe_4 has a Sn-excess of 26.4%. With respect to Te both alloys have a little deficiency that is less than the experimental error. These deviations from stoichiometry must be studied in relation to a better understanding of the phase diagrams of these alloys, research that is only just now beginning.

Finally, the optical energy gaps were obtained by Optical Diffuse Reflectance UV/VIS/NIR Spectroscopy. Optical diffuse reflectance data were collected for ground samples of Cu_2GeTe_4 and Cu_2SnTe_4. The spectra exhibit absorption edges indicative of narrow bandgap semiconductors in agreement with their black color, see Figure 5. Tails commonly observed on optical absorption edges originate from defects within the crystal structure that induce defect states in the electronic band structure. These defect states near the valence band maximum and conduction band minimum create a smearing of the band edge that is termed the Urbach tail [[2]8-29]. When estimating the bandgap of a semiconductor it is proper to model the Urbach tail and exclude this region from the fitting of the band edge when determining the bandgap [[30]]. The Urbach tail appears as a linear region at the low energy region of the absorption edge when the log of the absorption is plotted as a function of energy [26]. Fitting the slope of this linear region yields the Urbach energy, which was determined to be 0.288(1) eV and 0.3795(5) eV for Cu_2GeTe_4 and Cu_2SnTe_4 respectively.

In semiconductor compounds, bandgaps may be of direct or indirect origin, depending on the location(s) of the valence band maximum and the conduction band minimum in k-space. Direct bandgap materials exhibit relatively sharp absorption edges, while indirect bandgap compounds present a more gradual onset of the absorption edge [28]. In order to determine the nature of the bandgap transition in the compounds presented here, the optical absorption edge data, for energies greater than those determined for the Urbach tail region, were fit to the function for a direct bandgap semiconductor, $\alpha = A(E-E_g)^{1/2}/E$, and to the function for an indirect bandgap semiconductor, $\alpha = A(E-E_g)^2/E$, where A is a constant, E is the photon energy in eV, and E_g is the band gap energy [28]. Based on these fits, it was found that the absorption edge of Cu_2SnTe_4 showed a larger range of linearity using the direct function rather than the indirect function. Accordingly, Cu_2SnTe_4 is assigned a direct bandgap of 0.63 eV, which corresponds to ~1970 nm in the near infrared region of the electromagnetic spectrum. We are hesitant to definitely designate the bandgap of Cu_2GeTe_4 as direct or indirect, since the band edge lies near the end of the range of our instrument. However, Cu_2GeTe_4 appears to have a direct transition and fitting with the function for a direct bandgap yields 0.53 eV, which corresponds to ~2339 nm.

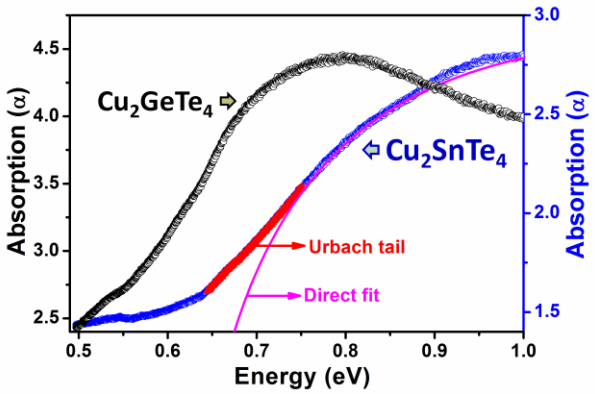

Figure 5. Diffuse reflectance UV-vis-NIR spectra for Cu_2GeTe_4 and Cu_2SnTe_4. The data for Cu_2SnTe_4 were fit using Tauc's function [[34]] for a direct-gap semiconductor, while the Urbach tail region (labeled) was excluded from the fitting of the absorption edge. The direct fit is shown with a thin solid curved line.

Telluride compounds in general can be semiconducting or metallic depending upon their composition and structure. The bandgaps reported here are narrower than those of some telluride compounds, such as CdTe, E_g~1.5 eV [28], an ideal value for use in solar cells. On the other hand,

Cu_2SnTe_4 and Cu_2GeTe_4 possess wider bandgaps than some other tellurides such as PbTe [28], $RbHgSbTe_3$ [31], $BaBiTe_3$[32] and Bi_2Te_3 [32], which all have E_g<0.5 eV. $CdAgTe_3$ possess E_g=0.65 eV [33], which is very close to that of Cu_2SnTe_4.

4. CONCLUSIONS

Polycrystalline samples of Cu_2GeTe_4 and Cu_2SnTe_4 alloys were prepared by the melt and anneal technique. Both alloys crystallize in an orthorhombic structure together with traces of a Cu_2Te secondary phase. The melting transition of Cu_2GeTe_4 was congruent whereas Cu_2SnTe_4 melts incongruently. While both alloys present large stoichiometric deviations for the cations Cu, Ge and Sn, the stoichiometry of the anion, Te, is close to the nominal composition. The band-gaps are located in the near-IR region of the electromagnetic spectrum. In view of the results these alloys could have applications as detectors in the near infrared radiation.

5. ACKNOWLEDGEMENTS

The Venezuelan authors want to thanks to CDCHTA-ULA grant C-1885-14-05-B.

6. REFERENCES

[1]. Berger, L.I. and Prochukhan V.D. *"Ternary Diamond-like Semiconductors"*. Consultants Bureau, New York, 1969, pp. 55-63.

[2]. Hamakawa, Y. *"Thin-film Solar Cells: Next Generation Photovoltaics and its Applications"*. Springer-Verlag Berlin Heidelberg (2004).

[3]. Adelifard, M., Mohagheghi, M.M.B. and Eshghi, H., Phys. Scr. 2012; **85**: 035603.

[4]. Kuku, T.A. and Fakolujo O.A., Solar Energy Materials 1987; 16: 199–204.

[5]. Kuku T.A. and Fakolujo O.A., Proceedings of the 3rd International Symposium on Optical and Optoelectronic Sciences of Engineering 14-18 April, 1986. Innsbruck, Austria. SPIE Vol. 653 pp.321-325, (1986).

[6]. Tiwari, D. and Chaudhuri, T. K., Solid State Physics, Procceding of the 55th DAE Solid State Physics Symposium, 26-30 December 2010, Manipal, India. AIP Conference Proceedings, Vol. 1349, pp. 1295-1296.

[7]. Berg D.M, Djemour, R, Gütay, L, Zoppi, G., Siebentritt, S, & Dale, P.J., Thin Solid Films 2012: 520, 6291–6294.

[8]. Morelli, D.T. and E.J. Skoug. MRS Proceedings Spring Meeting; Symposium N: *"Materials and Devices for Thermal to Electric Energy Conversion"*. Vol. 1166, Editors: Yang J., Nolas G.S., Koumoto K., Grin Y. (2009).

[9]. Cho J.Y., Shi X., Salvador J.R., Meisner G.P., Yang J., Wang H.,Wereszczak A.A., Zhou X., and Uher C., Physical Review B 2011: 84: 085207.

[10]. Samanta L.K., Phys. Stat. Sol. (a) 1987 ; 100, K93.

[11]. Ibáñez, M., Cadavid, D., Anselmitamburini, U., Zamani, R., Gorsse, S., Li,W., López, A.M., Morante, J.R., Arbiol, J. and Cabot, A. J., Material Chemistry A 2013; 1421-1426.

[12]. Peña R., Grima-Gallardo P., Nieves L., Marcano G., Quintero M., Moreno E., Ramos M.A., Henao J.A. and Briceño J.M. Adv. Mat. Sci. & Technol. 2013; **7:** 23-38.

[13]. Berger L.I., and Kotina E.K. Inorg. Mater. 1973; **9**: 330-322.

[14]. Delgado G.E., Mora A.J., Pirela M., Velásquez-Velásquez A., Villarreal M. and Fernandez B.J. Phys. Stat. Sol. (a) 2004; 201: 2900-2904.

[15]. Villarreal M., Fernandez B.J., Pirela M. and Velásquez-Velásquez A. Revista Mexicana de Física 2003; 49 Suplemento 3: 198-200.

[16]. Delgado G.E., Mora A.J., Marcano G. and Rincon C. Cryst. Res. Technol. 2008; 43: 433-437.

[17]. Sharma B.B., Ayyar R. and Singh H. Phys. Stat. Sol. (a) 1977; 40: 691.

[18]. Dovletov K. and Tashliev K. Izv. Akad. Nauk., Turkm. SSR, Ser. Fiz.-Tekhn., Khim. Geol. Nauk 1978; 2: 24-27.

[19]. Palatnik L.S., Komnik Yu. F., Koshkin, V.M. and Belova E.K. Dokl. Akad. Nauk. SSSR 1961; 137: 68-71.

[20]. Rivet J. Bull. Soc. Chim. Fr. 1963; 12: 2703.

[21]. Averkieva G.K., Vaipolin A.A. and Goryunova N.A. Sov. Research in New Semiconductor Materials 1965; 26-34.

[22]. Rivet J. Ann. Chim. (Paris) 1965; 10 (5-6); 243-270.

[23]. Carcaly C., Rivet J. and Flahaut J.J. Less-Common Met. 1975; 41(1): 1-18.

[24]. Carcaly C., Rivet J. and Flahaut J.J. Less-Common Met. 1977; 51(1): 165-171.

[25]. Kubelka P., Monk F., Z. Technol. Phys. 1931; 12: 593–601.

[26]. Urbach F., Phys. Rev. 1953; 92 : 1324.

[27]. Boultif A. and Louër D. J. Appl. Cryst. 1991; 24: 987-993.

[28]. Pankove J. I., Optical Processes in Semiconductors, Dover Publication, New York, 1971.

[29]. Choudhury B., Dey M., Choudhury A., Int. Nano Lett. 2013; 3: 25.

[30]. Malingowski A. C., Stephens P. W., Huq A., Huang Q., Khalid S., Khalifah P. G., Inorg. Chem. 2012; 51: 6096-6103.

[31]. Li J., Chen Z., Wang X., Proserpio D. M. J. Alloy Compds. 1977; 262-263: 28-33.

[32]. Chung D.-Y., Jobic S., Hogan T., Kannewurf C. R., Brec R.; Rouxel J., Kanatzidis M. G. J. Amer. Chem. Soc. 1997; 119: 2505-2515.

[33]. Li J., Guo H.-Y, Zhang X., Kanatizidis M. G., J. Alloys Compds. 1995 ; 218: 1-4.

[34]. Tauc J.. MRS Bull. 1969; 3: 37-46.